Dynamic molecular structure and phase diagram of DPPC–Cholesterol binary mixtures: A 2D-ELDOR study

ARTICLE *in* THE JOURNAL OF PHYSICAL CHEMISTRY B · OCTOBER 2007

Impact Factor: 3.3 · DOI: 10.1021/jp0732110 · Source: PubMed

3 AUTHORS, INCLUDING:

Yun-Wei Chiang
National Tsing Hua University
27 PUBLICATIONS **482** CITATIONS

SEE PROFILE

Antonio J Costa-Filho
University of São Paulo
83 PUBLICATIONS **1,024** CITATIONS

SEE PROFILE

Dynamic Molecular Structure and Phase Diagram of DPPC−Cholesterol Binary Mixtures: A 2D-ELDOR Study

Yun-Wei Chiang,[†] Antonio J. Costa-Filho,[‡] and Jack H. Freed*

Baker Laboratory of Chemistry and Chemical Biology, and National Biomedical ACERT Center for Advanced ESR Technology, Cornell University, Ithaca, New York 14853-1301, U.S.A.

Received: April 25, 2007; In Final Form: July 10, 2007

This paper is an application of 2D electron−electron double resonance (2D-ELDOR) with the "full Sc− method" to study model membranes. We obtain and confirm the phase diagram of 1,2-dipalmitoyl-*sn*-glycerophosphatidylcholine (DPPC)−cholesterol binary mixtures versus temperature and provide quantitative descriptions for its dynamic molecular structure using 2D-ELDOR at the Ku band. The spectra from the end-chain 16-PC spin label in multilamellar phospholipid vesicles are obtained for cholesterol molar concentrations ranging from 0 to 50% and from 25 to 60 °C. This phase diagram consists of liquid-ordered, liquid-disordered, and gel phases and phase coexistence regions. The phase diagram is carefully examined according to the spectroscopic evidence, and the rigorous interpretation for the line shape changes. We show that the 2D-ELDOR spectra differ markedly with variation in the composition. The extensive line shape changes in the 2D-plus-mixing-time representation provide useful information to define and characterize the membrane phases with respect to their dynamic molecular structures and to determine the phase boundaries. The homogeneous T_2's are extracted from the pure absorption spectra and are used to further distinguish the membrane phases. These results show 2D-ELDOR to be naturally suitable for probing and reporting the dynamic structures of microdomains in model membrane systems and, moreover, providing a very detailed picture of their molecular dynamic structure, especially with the aid of the "full Sc− method".

Introduction

The present report is the first of two papers investigating the dynamic molecular structure of phase domains in model and biological membrane systems using 2D-ELDOR (electron−electron double resonance) techniques with the aid of the newly developed "full Sc− method".[1] This method is a new fitting strategy, which utilizes the full complex signal instead of just the magnitude. It accomplishes this by accurately correcting the raw signals for the inherent phase distortions. This also enables the recovery of the spectrum in the pure absorption mode. The spectral resolution is, therefore, significantly improved over the much broader magnitude spectra.

In the present report, we investigate the phase diagram of a binary mixture of DPPC−cholesterol over a range of cholesterol mole concentrations, [Chol], from 0 to 50% and temperatures from 25 to 57 °C using the full Sc− method. This phase diagram has previously been investigated using several physical techniques, and it was shown that there are three membrane phases, the gel, liquid-ordered (L_o), and liquid-disordered (L_d) phases, which exist in distinct phases and/or coexist. However, the phase boundaries as well as the phase coexistence regions were not determined consistently in these studies and were found to depend on the physical methods employed, as we will discuss below. We chose this phase diagram to study because it contains both single phases and phase coexistences, which are of interest to membrane biophysicists, and because it had posed a challenge (discussed below) to continuous-wave (cw)-ESR. Thus, we felt that a more powerful experimental technique was required. In another paper,[2] we report on the study of the dynamic molecular structure of plasma membrane vesicles (PMV) and membrane structural changes caused by antigen cross-linking of IgE receptors on the cell surface using the full Sc− method. These two papers demonstrate that 2D-ELDOR with the aid of the full Sc− method is a valuable and powerful tool to study dynamic molecular structures in model and biological membranes.

Microdomains are believed to exist in plasma membranes[3−7] and isolated membrane vesicles, as studied by various physical techniques. They are believed to be dynamic in terms of domain size and lipid composition and may not have distinct phase boundaries. However, by studying model membrane systems whose phases are analogous to the main components in biomembranes, some insight into the complex phase environment of biomembranes may be achieved. A method that is sensitive to probing membrane domains and able to provide quantitative insight into the dynamic molecular structure is highly desirable.

The phase diagram of the DPPC−cholesterol system with temperature (20−60 °C) contains a variety of membrane phases. It has been studied using such physical methods[8] as X-ray diffraction (XRD),[9,10] cw-ESR,[11] fluorescence correlation spectroscopy (FCS),[12] fluorescence resonance energy transfer (FRET),[13] NMR,[11,14−18] and differential scanning calorimetry (DSC).[16,17,19] However, the determination of a complete diagram required more than one method to investigate the large compositional space and temperature range, and discrepancies still exist. Table 1 shows a summary of several versions of the DPPC−cholesterol boundaries of the phase diagram, which were

[‡]Present address: Instituto de Física de São Carlos, Departamento de Física e Informática, Universidade de São Paulo, C.P. 369, CEP 13560−970, São Carlos, SP, Brazil.

[†]Present address: Department of Chemistry, National Tsing Hua University, Hsinchu, 30013, Taiwan.

10.1021/jp0732110 CCC: $37.00
Published on Web 08/31/2007

TABLE 1: Summary of DPPC−Cholesterol Phase Boundaries from Several Studies [j]

temp.	ref	gel → gel/L_o	gel/L_o → L_o	L_d → L_d/L_o	L_d/L_o → L_o	L_d → L_o
23−25 °C	*a*	20%	30%			
	b	16%	25%			
	e	3%	35%			
	f	5%	20%			
	g	8%	23%			
	i	18%	32%			
35 °C	*c*	7%	23%			
	d	8%	23%			
	e	5%	23%			
	f	5%	20%			
	g	8%	30%			
	i	>20%	<30%			
48 °C[e]	*e*					35%
	f					20%
	g			8%	30%	
	i			12%	28%	
57 °C[e]	*e*					40%
	f					30%
	g			15%	30%	
	i			12%	28%	
60 °C[b]	*h*			15%	30%	

[a] Korlach[12] (2005); FCS. [b] Feigenson[13] (2001); FRET. [c] Vist[16] (1990); ^{2}H NMR, DSC. [d] Ipsen[17] (1987); compilation of NMR, DSC, EM, ESR data; theory. [e] Huang[14] (1993); ^{2}H; ^{13}C NMR. [f] McMullen[19] (1995); DSC. [g] Sankaram[11] (1991); ^{13}C, ^{2}H NMR, DSC, XRD, biradical ESR, theoretical calculations. [h] Cao[15] (2005); NMR. [i] Chiang (2007; the present report); 2D-ELDOR. [j] Note: The percentage shown indicates the overall cholesterol concentration [Chol].

mainly determined using the methods mentioned above. (Note that the phase diagram deduced mainly from the XRD results is not listed since it was mostly obtained from aligned lipid mixtures, in which the phase behavior is found to be somewhat different from that of membrane vesicles.) The phase boundaries determined from the present study are shown in shaded lines and discussed in later sections. Overall, a number of discrepancies in the phase boundaries are observed in the phase diagram over temperature from 25 to 60 °C. At lower temperatures, the tilted gel phase is observed in the region with [Chol] < 8% in most studies. At higher temperatures, the L_o and L_d phases and their coexistence are reported, but the determinations of the boundaries are not consistent. The discrepancies might be because each method has its own (optical or spectroscopic) resolution and sensitivity limits in probing dynamic local domains in a membrane system. Thus, a full determination of the phase diagram calls for more than one method. It would thus be desirable to have a single technique which is suitable and sensitive enough for probing phase domains in membranes over a large range of composition and temperature.

The determination of the DPPC−cholesterol phase diagram has also posed a challenge using standard spin-label cw-ESR. Figure 1 shows a series of X-band cw spectra collected from 16-PC in multilamellar membrane vesicles of DPPC−cholesterol binary mixtures with a range of [Chol] at 23 °C. While most studies (not using ESR) show that there is a two-phase coexistence region along this range of compositions, the cw spectra and our analysis show a continuous variation of a wide range of [Chol], which goes from the gel (low cholesterol region) to the L_o phase. That is, the line shape changes are continuous, providing no evidence. This is contrary to our previous cw-ESR study of binary mixtures of DPPC−DLPC.[20] In that study, significant line shape changes could be observed after just a small amount of DLPC was added to pure DPPC, that is, the phase transition from the tilted gel to the gel. Also, it was possible to distinguish the gel-to-liquid disordered phase transitions by cw-ESR because of the substantial spectral differences between these phases. However, we find it difficult to use cw-ESR to distinguish the more subtle phase transition from gel to L_o. One problem with cw-ESR is that the presence of large line broadening, such as inhomogeneous broadening (IB) due to unresolved proton hyperfine and local heterogeneity, reduces the spectral resolution. A more advanced and powerful technique is required.

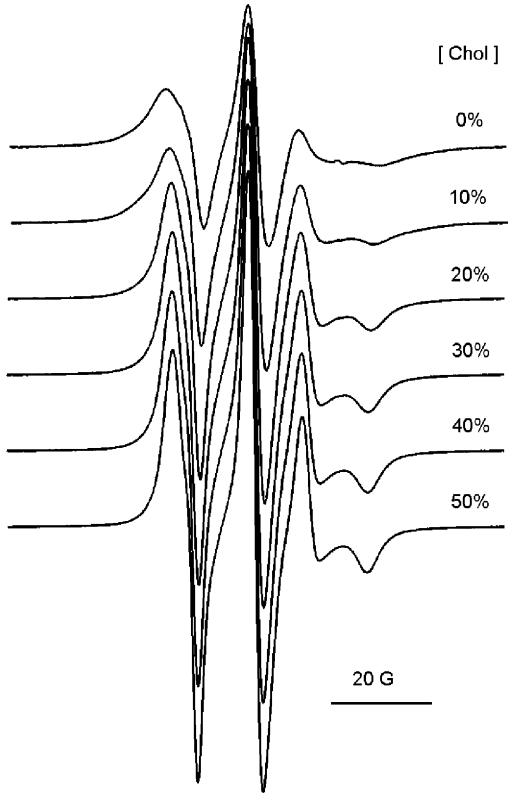

Figure 1. The cw-ESR spectra of 16-PC collected at 9.3 GHz from multilamellar membrane vesicles of DPPC−cholesterol mixtures at 23 °C.

In the present report, we demonstrate from experimental data as well as from the rigorous interpretation of the spectral line shape simulations that 2D-ELDOR, especially with the full Sc− method of analysis, is an appropriate and powerful technique for determining the phase diagram of the DPPC−cholesterol system over a large temperature range while at the same time providing detailed insight into the molecular dynamics and structure characterizing the membrane phases.

Materials and Methods

Materials and Sample Preparations. The phospholipids 1,2-dipalmitoyl-*sn*-glycerophosphatidylcholine (DPPC) and the spin label 1-palmitoyl-2-(16-doxylstearoyl) phosphatidylcholine (16-PC) were purchased from Avanti Polar Lipids, Inc. (Alabaster, AL). Cholesterol was obtained from Nu Chek Prep (Elysian, MN). Purity >99.5% was established by thin-layer chromatography on Adsorbosil Plus 1 silica plates from Alltech Associates. All materials were used without further purification.

Measured stock solutions of the lipids in chloroform were mixed in a glass tube. The concentration of spin label was 0.5 mol % of the lipids for all samples. Upon evaporation of the solvent by N_2 flow, the lipids formed a thin film on the wall of the tube. Then, the samples were evacuated with a mechanical pump overnight to remove trace amounts of the solvent. After the addition of 2 mL of 50 mM Tris (pH 7.0), 160 mM sodium chloride, and 0.1 mM EDTA, the lipids were scraped off of the wall, and the solution was stirred for 1 min and kept in the dark at room temperature for at least 2 h for hydration. Samples were then pelleted using a desktop centrifuge and transferred to a 1.5 mm inner diameter capillary. Samples were deoxygenated in a glove bag by alternately pumping and adding N_2 gas over 3 h. Each capillary was sealed with paraffin.

The cw-ESR spectra were collected on a Bruker Instruments EMX ESR spectrometer at a frequency of 9.3 GHz at room temperature (~23 °C).

2D-ELDOR Measurements. 2D-ELDOR experiments were performed using the 2D-FT-ESR spectrometer[21] at the Ku band frequency (ca. 17.3 GHz). Three 4 ns $\pi/2$ pulses were used in the experiments. Typical dead times in the present study were approximately 35 and 28−37 ns, respectively, for t_1 and t_2. Instrumental details can be found elsewhere.[22−24] In a brief summary, one collects the free induction decay (FID) signal after the third pulse along t_2 for a series of settings of the time, t_1, which represents the time between the first two pulses; t_1 is stepped out with 128 steps of 2 ns each. Each FID, which corresponds to an individual t_1 step, is collected along t_2 with a step size of 1 ns for a total of 256 data points. The 2D-FT-ESR spectrum in the frequency domain (f_1 vs f_2) is then constructed by Fourier transforming with respect to t_1 and t_2. The time between the second and third pulses is referred to as the mixing time, T_m. It provides an additional dimension to the 2D-ELDOR experiment, wherein one observes how the intensities of the spectral peaks (cross and auto peaks) develop versus T_m. Various molecular mechanisms can be separated and revealed from the variety of line shape changes in such an experiment.[25,26] Two distinct complex signals, called Sc− and Sc+, are obtained. However, the Sc+ signal is less useful than the Sc− signal because it usually decays too rapidly during the spectrometer dead time.[1] Therefore, Sc−(f_1, f_2) has been the main signal used in 2D-ELDOR analysis.[1]

The Full Sc− Method and the Absorption Line Shapes. A new spectral analysis method called the "full Sc− method" has recently been developed.[1] Instead of performing spectral fitting using the magnitude of the complex Sc−(f_1, f_2) data to avoid complications from phase distortions, the real and imaginary parts of the Sc− signal are simultaneously fit. This modification in the fitting strategy benefits from the greater resolution over the magnitude mode. (It also doubles the number of spectral fitting points.) In addition, it provides the phase corrections needed to correct for the experimental phase distortions, such as those from imperfect spectral bandwidth coverage and pulse shapes. The phase distortions can be avoided by displaying the spectrum in the magnitude mode but at the expense of sacrificing the resolution. We find that by using the full Sc− method, we significantly reduce the ambiguity in the fitting parameters. An additional feature we use is to simultaneously fit both the ELDOR and SECSY-formatted spectra in the full Sc− domain, wherein each format emphasizes different details of the fitting. Once the phase corrections are obtained, it is possible to (approximately) convert the experimental data to the pure absorption mode. The absorption spectrum shows the improved spectral resolution and thus provides several advantages. For example, the absorption spectrum is characterized by sharper and narrower lines as compared to the spectrum in the magnitude mode. When being displayed in the SECSY format, it provides the homogeneous broadening (HB) separately from the inhomogeneous broadening (IB), showing them along the f_1 and f_2 directions, respectively. The line shapes in the f_1 direction are of a simple absorption type, that is, Lorentzians, whose widths are given by the real part of the eigenvalues representing the dynamic spin packets. Details for the procedure of obtaining the pure absorption spectrum can be found elsewhere.[1]

Spectral Simulations and Nonlinear Least-Squares Fitting. The 2D-ELDOR spectral fitting was performed using the nonlinear least-squares fitting program, NLSPMC-fullscm, which was modified from Budil et al.[27] for full Sc− fitting. The theory underlying this program was developed using the Stochastic Liouville equation (SLE).[28−30] The dynamic parameters were obtained in the spectral fitting and used to describe the dynamic molecular structure of lipid membranes.[20,31] Among the most important are $R_\perp$ and $R_\parallel$, the principal values of an axially symmetric rotational diffusion tensor, which characterizes the dynamics of the acyl chain, for the nitroxide moiety attached to the chain segment, and the order parameters, S_0, which represent the extent of alignment of the acyl chain with respect to the local director axis and S_2, which measures the asymmetry in alignment.

The spectral simulations for membrane vesicles used in the NLSPMC-fullscm program were obtained with the model of microscopic order with macroscopic disorder (MOMD), that is, the lipids in the membrane are microscopically well-aligned within the vesicles but with the macroscopic directors isotropically distributed so that there is no macroscopic ordering.[28,32] In other words, the spectrum is a sum of the spectra for all orientations with respect to the direction of the magnetic field.

The quality of fit was objectively and quantitatively evaluated in the nonlinear least-squares fitting, which minimizes the chi-square (χ^2) as previously discussed for 2D-ELDOR in the magnitude mode,[27] except now, the full Sc− data set is utilized. (Note that the existence of negative lobes does not interfere with the chi-square analysis since the absolute value of the difference between the simulated and experimental data is used.) Indeed, we find that the phase corrections enable excellent quality of fit to a range of experimental data.[1] This is also supported by previous analysis of the effects of finite dead times[33] and of the effects of pulses of finite width.[34,35]

The Homogeneous Relaxation Time, T_2. Studies of the homogeneous relaxation time T_2 have been very useful in studying molecular dynamics. In the past, the T_2's of the different hyperfine lines have been studied in both the motionally narrowed and the slow-motional regimes.[25,36] The homogeneous line widths (i.e., T_2^{-1}) are determined by the rotational modulation of the hyperfine and g tensors, as well as line broadening independent of these interactions (e.g., Heisenberg spin exchange and spin-rotational relaxation), which is denoted as the residual homogeneous line width, T_{2edi}^{-1}. This line width term (i.e., T_{2edi}^{-1}) is an additional parameter that is determined in the full Sc− spectral fitting.

There have been three main ways used in processing pulsed ESR signals to extract homogeneous line widths from slow-motional experimental data. One is to perform a 2D field-swept electron-spin−echo (ESE) experiment to study T_2 variations across the spectrum.[37,38] However, because the 2D-field-swept ESE experiment requires an order-of-magnitude longer acquisition time in comparison with that of the 2D-Fourier transform (FT)-ESR experiments, it has been rarely employed in recent years.

The second method is to perform a FT two-pulse ($\pi/2-\pi/2$) correlation spectroscopy (COSY) experiment to collect the variation of the T_2's. It is useful to apply a "shearing transformation (i.e., one replaces t_2 with $t_1 + t_2$ for the $t_2 > t_1$ data,) to transform the COSY data to the spin−echo-correlated spectroscopy (SECSY) format. After Fourier transforming the data in the SECSY format along the t_2 direction, the homogeneous T_2's are revealed as exponential decays in the t_1 direction and are able to be obtained by fitting Lorentzians, which are referred to as "dynamic spin packets" distributed under the line shape envelope in the t_1 direction. Alternatively, one obtains the homogeneous line widths along f_1 after a FT of $t_1 \rightarrow f_1$.[22,39]

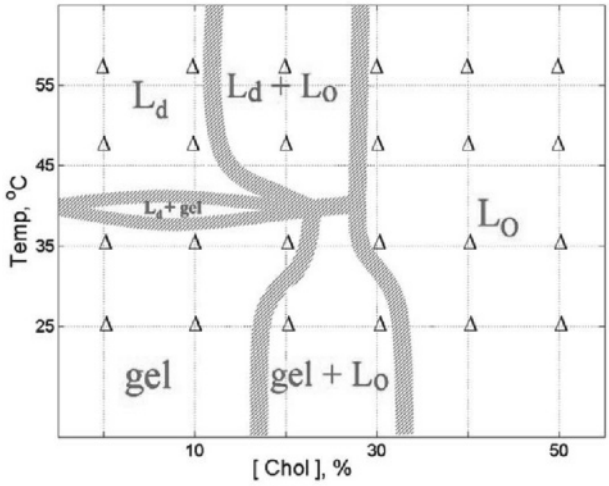

Figure 2. The DPPC−cholesterol phase diagram determined using 2D-ELDOR. The samples shown in the present report are marked by triangles. The membrane phases, the coexistence regions, and the phase boundaries are determined based on the 2D-ELDOR spectroscopic evidence and the dynamic parameters obtained from the spectral fitting using the full Sc− method.

Saxena and Freed[33,40] show that this is best done after obtaining the pure absorption since this information is obscured in the magnitude format.

The third method for determining homogeneous line widths is to use the 2D-ELDOR spectra in the SECSY format, and again, it is strongly advised to use the pure absorption mode,[33,40] which requires that the phase distortions in experimental data be corrected.[1] Saxena and Freed[40] have demonstrated that homogeneous line widths are better obtained using this three-pulse method because it is much more effective in filtering baseline anomalies than the two-pulse sequence in the COSY experiment (i.e., the second method). One merely uses a small T_m so that the 2D-ELDOR signal is strong. In some cases, it is useful to study how the homogeneous line width varies with T_m.[22,39,41]

In the present report, we use the third method to extract the homogeneous line widths from the absorption spectra.

Results and Discussion

The Phase Diagram of DPPC−Cholesterol with Temperature Variation. The phase diagram of a binary mixture of DPPC−cholesterol, which we have determined in the present study, is shown in Figure 2. There are three relevant membrane phases, that is, the gel, L_o, and L_d, as well as two-phase coexistence regions. The compositions and temperatures, for which we collected 2D-ELDOR spectra, are marked by small triangles. We performed the experiments at four different temperatures, that is, at 25, 35, 48, and 57 °C, with six samples covering the range of [Chol] from 0 (i.e., pure DPPC) to 50%. The bold-patterned lines indicate the phase boundaries that we determined, as described below. There are uncertainties, which are about 5% in compositional variation,[20] for the boundary widths in the phase diagram.

2D-ELDOR Provides Distinct Pattern Recognition for Three Different Membrane Phases. 2D-ELDOR provides great sensitivity to the dynamics and the microscopic ordering through its range of line shape changes. Visual inspection shows distinct differences in the 2D-ELDOR spectra from the three phases, as shown in Figure 3. The mixing times, T_m of 50, 150, and 500 ns, are shown for each phase. The spectra for Figure 3a, b, and c are for the L_d, L_o, and gel phases, respectively. The lipid compositions and temperatures are noted in the figure. They correspond to three experimental points in the phase diagram in Figure 2. The magnitude spectra are shown for convenience. Even in the magnitude mode, they have distinctly different characteristics.

In the L_d phase (Figure 3a), all peaks are sharp and narrow. Cross peaks grow in substantially with increasing mixing time. In the L_o phase, shown in Figure 3b, the most distinguishing spectral features are the absence of cross-peak development, a broad middle auto peak, and the high-frequency auto peak remaining sharp and narrow, similar to that of the L_d phase. The gel phase spectra are shown in Figure 3c. They have much broader auto peaks than those of the L_o and the L_d phases. In addition, there is almost no development of cross peaks with mixing time. Also, the lowest-frequency auto peak, which can be observed in both the L_o and L_d phases, is very weak in the gel phase.

These respective features are characteristic of the 2D-ELDOR spectra we obtained in the L_d, L_o, and gel phases. Thus, they provide general guidelines for distinguishing these phases simply by pattern recognition when the 16-PC spin probe is used in Ku-band 2D-ELDOR. We summarize these observations as the following: (i) The most important spectral characteristic to distinguish L_d from L_o is that the cross peaks develop rapidly relative to mixing time in L_o; (ii) the three auto peaks can be observed in the two fluid phases (L_d and L_o); (iii) in the gel phase, the spectrum has broad line shapes, and the auto peak at the lowest-frequency is hardly visible; and (iv) in the highly ordered phases (gel and L_o), the cross peaks are suppressed. It has been previously shown[30,40] that the cross-peak development in 2D-ELDOR is due to magnetization transfer, arising from the intramolecular ^{14}N electron−nuclear dipolar (END) interaction. (The intermolecular Heisenberg spin-exchange (HE) interaction is also effective but not significant at the low spin-label concentrations used.) In a highly ordered environment, the range of orientational motion, which induces ^{14}N nuclear spin flips to transfer the spins from one hyperfine line to another, is more restricted. This, plus the fact that the enhanced MOMD effect on the IB is not effectively cancelled out for the cross peaks, results in the suppression of cross peaks in the spectrum.

Dynamic Molecular Structure of the Phases. In this section, we focus on the interpretation of the dynamic parameters obtained from the spectral simulations. These parameters are used (as discussed below) to help determine the phase diagram in Figure 2. All of the spectral fits are unambiguously obtained in both the ELDOR and SECSY formats using the full Sc− method and are shown in the Supporting Information (Figures S1 − S4). The dynamic and ordering parameters we obtained from the 2D-ELDOR spectral fitting are shown in Figure 4. Figure 4a and b, respectively, shows the results of the rotational diffusional rates ($R_\perp$ and $R_\parallel$) and Figure 4c and d the ordering (S_0 and S_2). Since $R_\perp$ and S_0 are determined to greater accuracy in the fitting, we will emphasize these results in the following analysis.

The Phase Diagram at 25 °C. Figure 2 shows that as the [Chol] increased from 0 to 50%, the sequence gel → gel + L_o → L_o was found. We now describe how this was determined.

Initially, all six compositions were fit under the assumption that there was only a single phase at each point. The initial results showed that the spectra of [Chol] = 20 and 30% has χ^2 values significantly higher than the others. Thus, the likelihood that they were in the two-phase gel + L_o region was studied using two-component fits to the 20 and 30% [Chol] cases. Each of these two cases was selected using the dynamic parameters

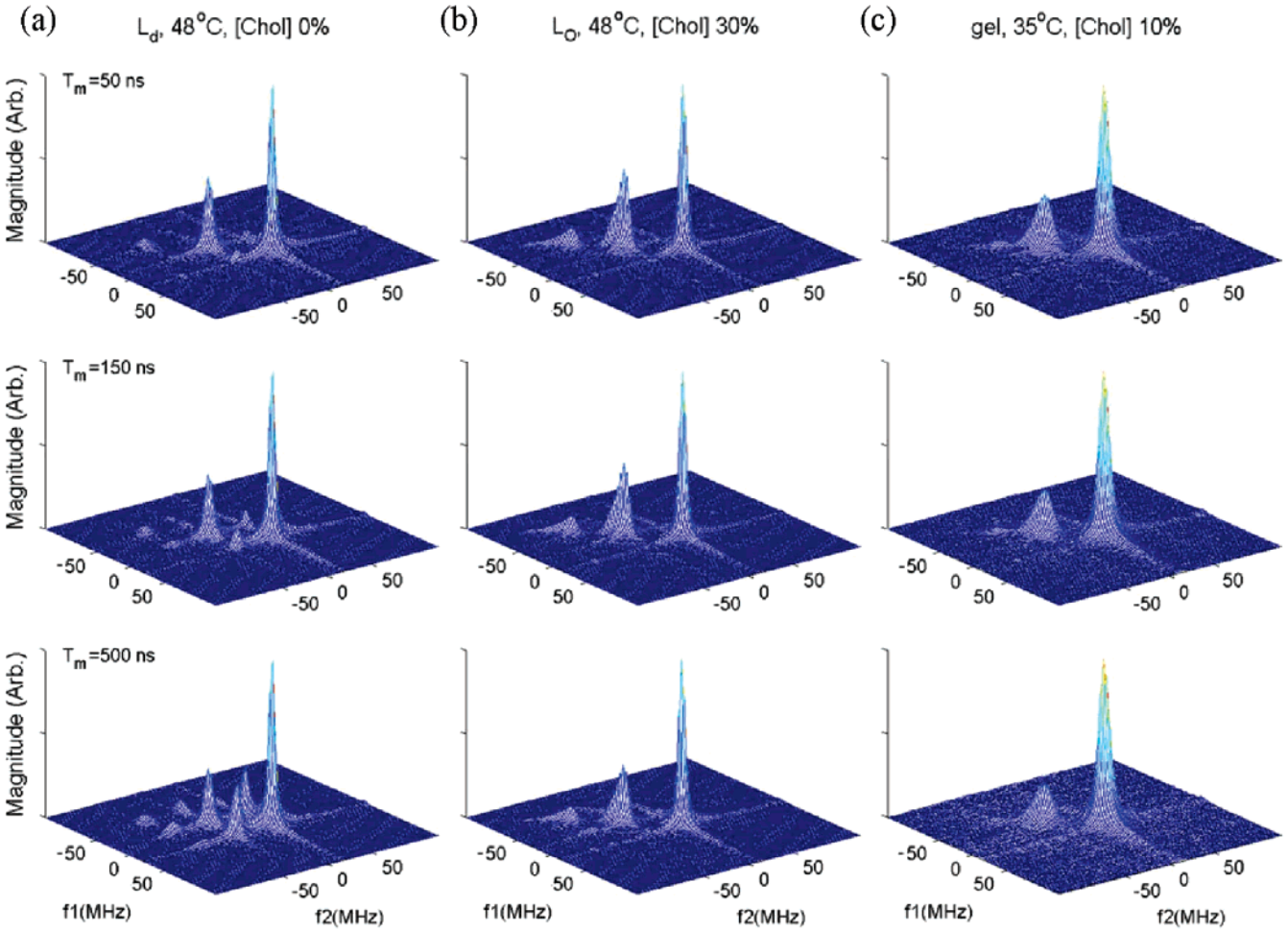

Figure 3. The 2D-ELDOR experimental spectra in the magnitude mode with three different mixing times in the (a) L_d, (b) L_o, and (c) gel phases. They display distinctly different spectra and provide clear pattern recognition for one to distinguish membrane phases by a visual inspection.

found for the 10% [Chol] in the gel phase and the 40% [Chol] in the L_o phase as seed values. Indeed, we achieved significantly better fits, where the final dynamic parameters were nearly identical (well within error limits) for both the 20 and 30% [Chol] cases, and the respective relative amounts of gel and L_o phases (85% gel and 15% L_o for 20% [Chol] and 10% gel and 90% L_o for 30% [Chol]) were consistent with the lever rule.[42] Thus, we concluded that the spectra within this two-phase region could be reconstructed using the same pair of spectral components. The lever rule could then be used to determine the phase boundaries.

When we examine the dynamic and ordering parameters $R_\perp$ and S_0 in Figure 4, we find that there is a significant increase in the former and a decrease in the latter when going from the gel to the L_o phase, as one would expect. (Similar comments apply to $R_\parallel$ and S_2.) These distinctions between the two phases are what lead to their characteristically different 2D-ELDOR spectra, as described above. We also note that these parameters show only a modest change within each phase. Within the coexistence region, the $R_\perp$ values for the gel phase and the L_o phase are 1.3×10^8 s^{-1} and 3.1×10^8 s^{-1}, respectively. The S_0 values are 0.38 and 0.30, respectively. These are not large differences, emphasizing the need for a high-resolution spectroscopy such as 2D-ELDOR to distinguish them successfully.

Our result for the 25 °C series is in good agreement with the phase boundaries determined using FCS[12] and FRET[13] (cf. Table 1). According to a molecular-level model presented in Feigenson et al.,[13] there is a critical cholesterol concentration of approximately 16%. Above this concentration, the lattice of the DPPC-ordered (i.e., gel) phase would have to rearrange by expanding the cross-sectional area of headgroups to provide shielding of additional cholesterol from water. This physical picture is consistent with the well-known "condensing effect".[13] The two compositionally distinct phase components persist well, as [Chol] is above approximately 16%, and become a single fluidic-ordered (i.e., L_o) phase as [Chol] is greater than 25−30%, as detailed above. Although the phase boundary for gel → gel + L_o was reported to be about 3−5% [Chol] using other techniques,[11,14,19] we consider the discrepancy, as reviewed in Feigenson et al.,[13] is due to the sensitivity of the employed tools to probing nanoscopic phase-domain scales.

The Phase Diagram at 35 °C. All of the spectra at 35 °C for the six different compositions were well fit by a single component. The phase diagram shown in Figure 2 is drawn in recognition of this fact. It is primarily the behavior of $R_\perp$ versus [Chol] (cf. Figure 4a), which suggests a modest phase transition between 20 and 30% [Chol]. S_0 remains nearly constant at 0.28 ± 0.03, with just a small increase as [Chol] increases (cf. Figure 4c). (Additional evidence coming from residual line widths is discussed below.) It may be appropriate to infer that the similarity of results between the gel and L_o phases indicates that these points on the phase diagram are near a critical point (which, however, is pre-empted by a phase transition). Given the subtlety of changes in this region, a more thorough study would be warranted.

The good quality of the fits at 20 and 40% [Chol] is shown in the Supporting Information (Figures S1 and S1). Although there is a 20% difference in [Chol], they are quite similar, with

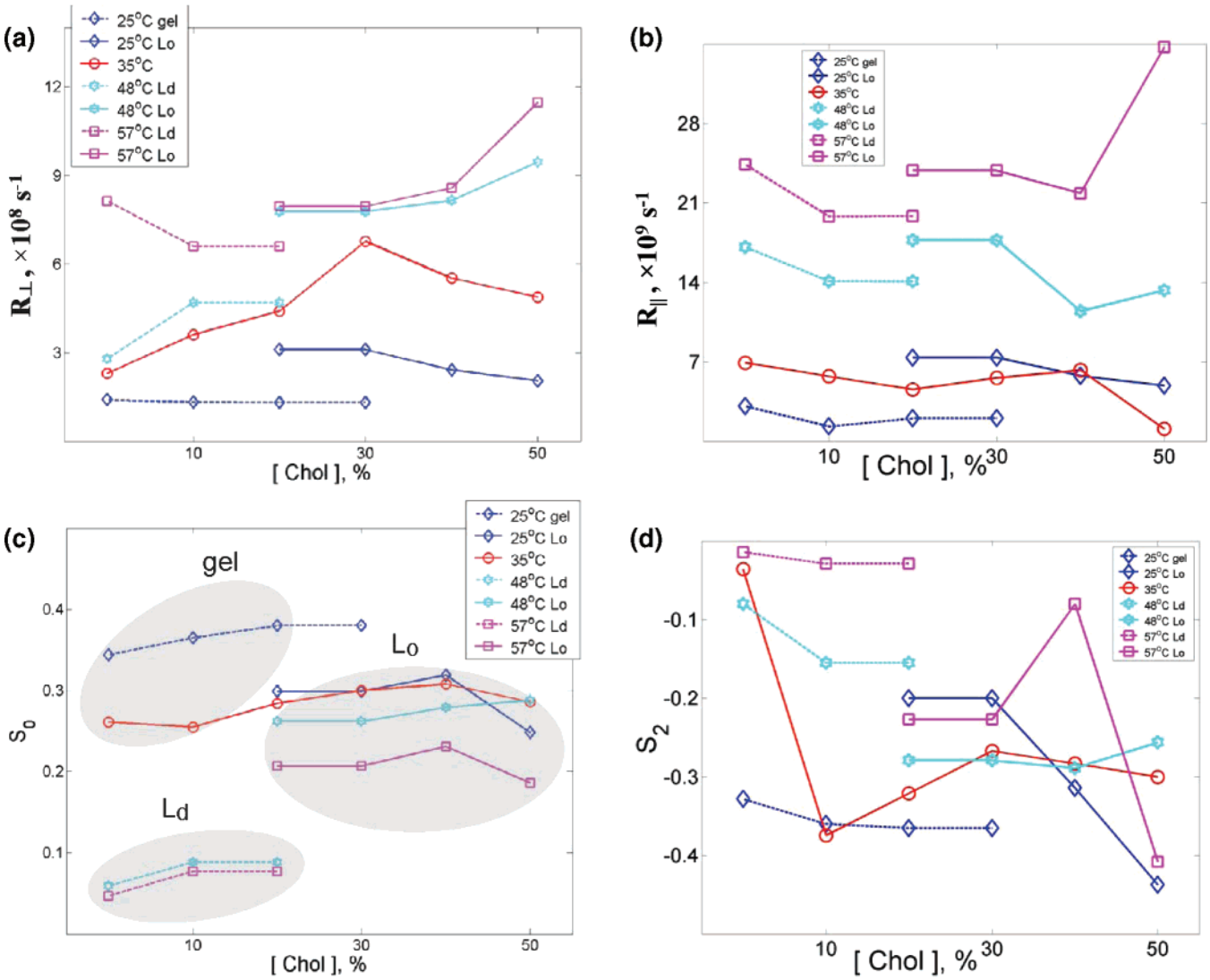

Figure 4. The dynamic parameters, which are obtained from the spectral fitting and provide a quantitative description of the overall dynamic molecular structure of the phases; the rotational diffusion coefficients $R_\perp$ and $R_\parallel$ are given in (a) and (b), respectively, while the order parameters S_0 and S_2 appear in (c) and (d), respectively.

only a few small differences. These figures show not only that very good fits were obtained by the full Sc− method, but the spectral line shape changes with [Chol] variation are the least distinct, as compared with those at the other temperatures studied.

Finally, we note that our results at 35 °C are consistent with earlier work showing there is a phase boundary, although its precise position was uncertain.[14,16−18]

The Phase Diagrams at 48 and 57 °C. The two-phase character at 20% [Chol] for 48 and 57 °C became clear primarily from fitting of the SECSY mode using the full Sc− method, which required two components for good fits. For 20% [Chol], we found a 45% L_d component (and a 55% L_o component) at 48 °C, and at 57 °C, it was 29% L_d and 71% L_o. The dynamic parameters $R_\perp$ and S_0 for 20% [Chol] were found to be very close to those obtained from the 10 and 30% [Chol] for the L_d and L_o phases, respectively, compare Figure 4a and c, suggesting phase boundaries nearby, as we have drawn in Figure 2 (although the vertical extrapolations of these boundaries would probably need to be modified by further more extensive studies, as suggested by the significant change in ratio of the L_o to L_d component in going from 48 to 57 °C). As expected, S_0 was significantly greater in the L_o versus L_d phase. We also found that $R_\perp$ was greater in the L_o phase, as previously reported.[6] The value of S_0 in the L_o phase showed considerable sensitivity to temperature as it decreased with increasing temperature; whereas in the L_d phase, it exhibited very little temperature dependence.

Figures S3 and S4 in the Supporting Information show that good fits are obtained at 48 and 57 °C, respectively, for the 20% [Chol]. We show in Figure 6 the two coexisting spectral components in the pure absorption mode (for just the $T_m = 500$ ns case) obtained from the fitting, which are used as basis spectra to fit the experimental spectra at 48 °C such as the one shown in Figure S3. The spectral features observed here are potentially useful as a reference to compare with $L_o + L_d$ coexistence in biological membranes.[1,6,7] The simulated pure absorption spectrum for $T_m = 500$ ns of the 10% [Chol] at 35 °C (i.e., gel phase) is also shown in Figure 6 for reference. The spectra displayed in the absorption mode show distinct differences for the three membrane phases.

Overall. The overall dynamic molecular structure of the phase diagram may then be mapped out in terms of the dynamic parameters as described above. We found the ordering S_0 to be the most informative and useful parameter for distinguishing and characterizing the different phases (cf. the shaded regions

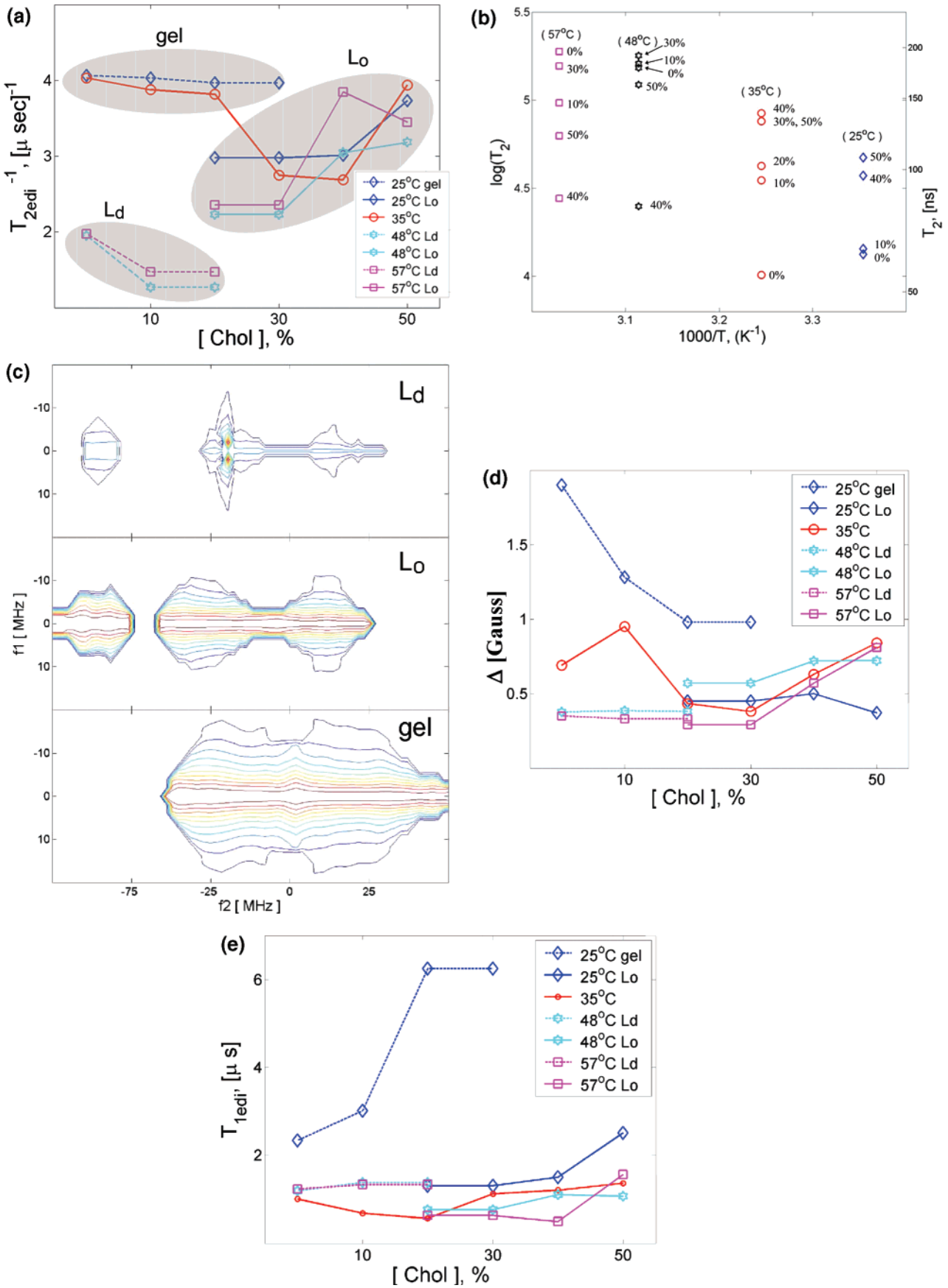

Figure 5. (a) The residual homogeneous line widths T_{2edi}^{-1}, obtained from spectral fitting, are found to be informative for characterizing each membrane phase. (b) The homogeneous T_2's, extracted from the pure absorption spectra, show a monotonic decrease with decreasing temperature. [These T_2's were measured for the high-frequency peak in each spectrum for $T_m = 50$ ns, with the variation in T_2^{-1} indicated in (c).] (c) The pure absorption spectra in the normalized contour mode; one can observe the homogeneous line widths in the f_1 direction. (d) The Gaussian inhomogeneous broadening, Δ. (e) The T_1's extracted from the 2D-ELDOR spectra versus T_m.

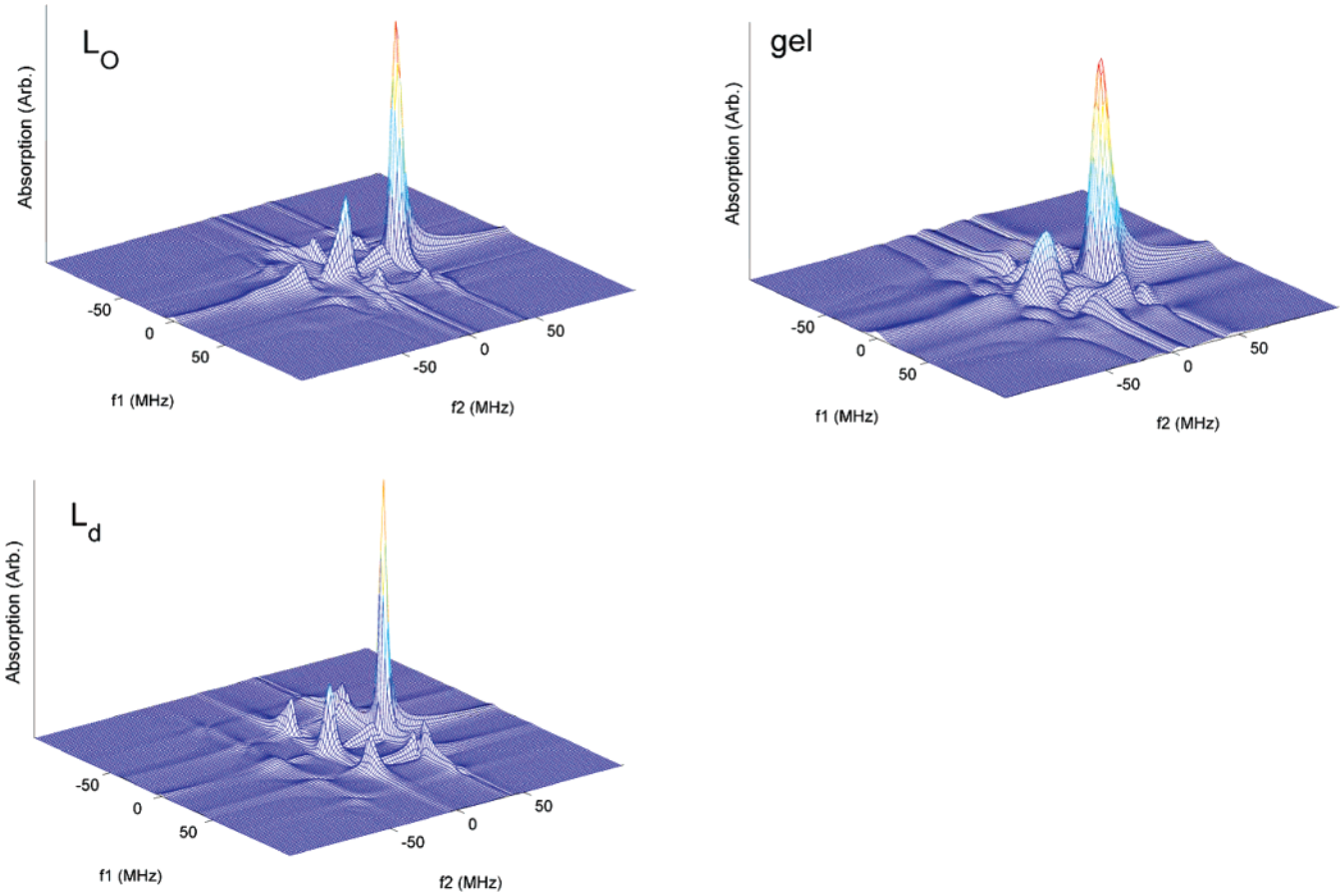

Figure 6. Simulated pure absorption spectral components, generated using the best-fit parameters in the full Sc− fitting of 20% [Chol] at 48 °C and T_m = 500 ns. The L_o and L_d spectra represent the components coexisting in the sample of 20% [Chol] at 48 °C and T_m = 500 ns, which corresponds to Figure S3. The gel spectrum, shown for comparison, is for 10% [Chol] at 35 °C and T_m = 500 ns. (Dead times used are the same as those in the experiments).

in Figure 4), although other parameters are useful. In the region of low [Chol], approximately <20%, the ordering S_0 shows a decreasing trend with increasing temperature, as expected. An abrupt decrease is observed as the temperature is increased from 35 to 48 °C, indicating the phase transition from gel to L_d. Many studies[11,14,16,19] of this phase diagram using other methods have previously reported that there is a phase transition from the gel phase to the L_d phase in the low [Chol] region as the temperature crosses 40 °C, as we have indicated in Figure 2. Of course, we would need more data points in this regime to accurately discern the phase boundary and presumed two-phase L_d + gel regime suggested in Figure 2. In the high [Chol] region, a single L_o phase is found to exist throughout the temperature range studied. In the region of high [Chol], approximately >30%, our results show that the S_0 values in the L_o region are ≥0.2, indicating the ordered environment. Overall, in the L_o region, the S_0 is found to gradually decrease with increasing temperature and is found to be rather insensitive to the [Chol] variation. Finally, we remind the reader that the dynamic parameters shown in Figure 4 provide quantitative descriptions for the respective membrane phases.

Membrane Phases Characterized by the Homogeneous Line Width, $1/T_2$. In addition to the dynamic parameters, which have been found useful and informative in characterizing membrane phases in many studies of spin-labeling ESR,[6,7,20,23,24] we found from the present study that T_2^{-1}, the homogeneous line width and therefore reports on the dynamics, provides additional distinctions between phases. Given that the ambiguity in the fitting parameters is greatly reduced by performing fitting in the full Sc− domain, T_2 and the residual homogeneous relaxation time, T_{2edi}, are reliably extracted from the experimental absorption spectra and from the spectral simulations, respectively, as described above.

TABLE 2: Homogeneous ($1/T_2$) and Residual Homogeneous ($1/T_{2edi}$) Line Widths (μs)$^{-1a}$

[Chol] temp.	0%	10%	20%	30%	40%	50%
57 °C	5.12	6.84	(1.47)	5.56	12.76	8.26
	(1.97)	(1.47)	(2.36)	(2.36)	(3.85)	(3.45)
48 °C	5.61	5.47	(1.27)	5.26	12.32	6.18
	(1.95)	(1.27)	(2.23)	(2.23)	(3.05)	(3.18)
35 °C	18.17	10.62	9.79	7.59	7.26	7.60
	(4.03)	(3.87)	(3.81)	(2.74)	(2.69)	(3.94)
25 °C	16.18	15.69	(3.97)	(3.97)	10.34	9.35
	(4.06)	(4.03)	(2.98)	(2.98)	(3.01)	(3.73)

[a] The $1/T_2$ and $1/T_{2edi}$ (in parentheses), respectively, are obtained from fitting Lorentzians to the recovered absorption spectra and from the full Sc− spectral fitting. Samples within the two-phase region are marked by two $1/T_{2edi}$ values, which represent the residual line widths for the two boundary components. The homogeneous T_2's are obtained from the spectra of the shortest T_m (50−150 ns) in the 2D-ELDOR experiments.

The homogeneous T_2's are obtained by fitting Lorentzians to the absorption spectra. In Table 2, we report the values of T_2^{-1} obtained from the spectra of the shortest T_m (50−150ns) obtained in the single-phase regions. The residual homogeneous line widths T_{2edi}^{-1}, which are obtained from the spectral fittings, are also given in Table 2 in parentheses. The results within the two-phase coexistence regions include two T_{2edi}^{-1} values, which represent the values for the pair of boundary spectra coexisting in the region. These T_{2edi}^{-1} are consistently much smaller than

the T_2^{-1}. This shows that the dominant contribution to the homogeneous line widths comes from the rotational modulation of the hyperfine and g-tensor interactions, as expected. (This contribution represents the difference between T_2^{-1} and T_{2edi}^{-1}.)

The T_{2edi}^{-1} are plotted in Figure 5a. One observes that they are unambiguously classified (cf. the shaded regions in Figure 5a) into three groups, which are consistent with the three membrane phases of Figure 2. The values of T_{2edi}^{-1} decrease in the order gel > L_o > L_d. In the gel phase, T_{2edi}^{-1} is insensitive to both temperature and [Chol] variation. In the L_d phase, T_{2edi}^{-1} decreases with increasing [Chol] and is much smaller, (ca. 2−3 times for the same temperature) than values in the gel and the L_o phases. T_{2edi}^{-1} in the L_o phase is found to be somewhat smaller than those in the gel and to increase moderately with increasing [Chol]. The three groups are distinctly different from each other. Such a collection of T_{2edi}^{-1} values provides an additional basis to characterize membrane phases. It is of interest to note that the T_{2edi}^{-1} values we obtained from biomembranes[2] [where we found that two major components (L_d vs L_o)] coexist in PMV, consistent with the present results for the respective L_d and L_o phases. (Note that a plot (not shown) of T_2^{-1} versus [Chol] also shows a distribution pattern, but a less distinct one, than the plot of T_{2edi}^{-1} in Figure 5a).

One of the advantages of using the full Sc− method is that pure absorption spectra can be reliably recovered with high resolution from the experimental data so that the homogeneous line widths, that is, T_2^{-1}'s, can be reliably obtained. Figure 5b shows the variation of log(T_2) with the inverse of temperature. Note that for Figure 5b, (i) the samples at the same temperature are denoted by the same marker; (ii) only the T_2^{-1}'s associated with samples in single phase regions are shown; and (iii) the percentage represents the [Chol]. Overall, the values of log(T_2) are found to linearly increase with increasing temperature. Figure 5c shows the normalized contour plots (see refs 1, 33, and 42 for definition) of the absorption spectra in (from top to bottom) the L_d, L_o, and gel phases, which respectively are from the samples of [Chol] = 0% at 57 °C, [Chol] = 40% at 48 °C, and [Chol] = 0% at 35 °C. The absorption spectra shown are the spectra of the longest mixing time, that is, T_m = 500 ns, and are displayed in the SECSY format. The homogeneous broadening occurs along f_1, whereas the spectrum (including inhomogeneous broadening) appears along f_2. By visual inspection, we see that these three membrane phases have distinctly different character, which makes these normalized contour plots very useful in visually distinguishing the respective phases. We may summarize our observations as follows. (i) The spectrum in the gel phase displays the broadest HB and only shows two peaks, respectively, at $f_2 \sim -25$ and 13 MHz. (ii) The spectrum in the L_o phase shows all three auto peaks and a narrower HB than in the spectrum from the gel phase. (iii) The narrowest and sharpest auto peaks are observed in spectrum of the L_d phase, indicating the longest T_2.

An additional line broadening parameter obtained in the fitting is the Gaussian inhomogeneous broadening, Δ. We plot the results for Δ in Figure 5d. In all cases, we find $\Delta > T_{2edi}^{-1}$. As was the case for T_{2edi}^{-1}, we find Δ decreases as gel > L_o, L_d, but the distinction between L_o and L_d is less clear. The large Δ for the gel phase, especially at 25 °C, is a major source of the poor resolution of the cw-ESR and 2D-ELDOR spectra in this phase. One may speculate that it is (partly) due to local inhomogeneities in the lipid bilayer that are (nearly) frozen out on the ESR time scale. One may further suggest that at least part of the T_{2edi}^{-1} results from incipient (but also) motional averaging of this inhomogeneity in the gel and L_o phases. Such matters may be worthy of further study.

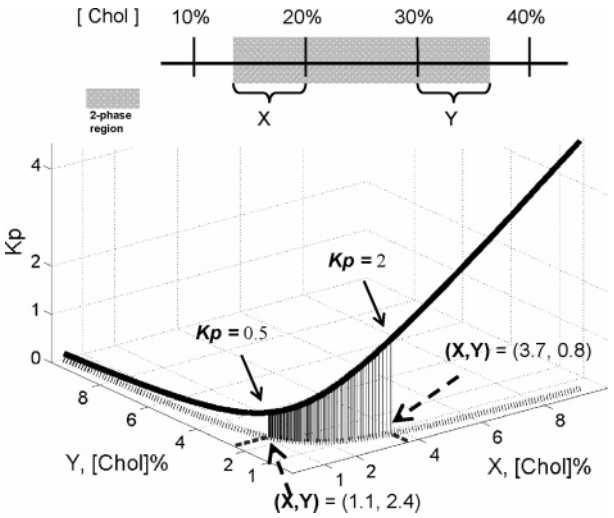

Figure 7. The calculations for the partition coefficient (K_p) of 16-PC within the phase coexistence of the gel and the L_o at 25 °C. The *X* and *Y* indicate the unknowns for the phase boundaries. A reasonable range for the K_p value is highlighted ($0.5 \le K_p \le 2$).

The 2D-ELDOR experiment also provides the spin−lattice relaxation time, T_1, which is obtained from the decrease in integrated signal with mixing time. We show the results for T_1 in Figure 5e. (Note there is considerable uncertainty in these values since they were obtained from three values of T_m.) The results for the gel phase at 25 °C are significantly larger than the others. We also find that $T_1 > T_{2edi}$ in all cases. At the higher-temperature L_d-to-L_o phase transition, one finds that T_1 decreases, and for the 25 °C gel-to-L_o transition, T_1 also decreases, but at 35 °C, this is reversed. Further study of T_1 (using a greater number of T_m) is also warranted.

Partitioning of the Spin Probe 16-PC. The discussion of the phase diagram so far was based on the simplifying assumption that the partition coefficient, K_p for the 16-PC spin probe is approximately unity in the two two-phase regions. This is a reasonable approximation based on previous studies. Chiang et al.[42] obtained a K_p for 16-PC in the gel + L_d coexistence region of the ternary mixture of DLPC/DPPC/Chol at 24 °C. It ranged from 1.1 for 0% [Chol] to 1.8 for 14% [Chol]; (here $K_p > 1$ prefers L_d over gel). Swamy et al. obtained a K_p for 16-PC in the L_o + L_d coexistence region of a ternary mixture of DOPC/SPM/Chol of 1.1 at 22 °C (here $K_p < 1$ prefers L_d over L_o). (These values of K_p typically have about a 30% uncertainty.) Thus, our above discussion with $K_p \sim 1$ is consistent with its measurement in related systems. Our present study involving 24 samples (cf. Figure 2) was sufficient to provide an overview of the phase diagram but is not extensive enough in the two-phase regions to provide useful independent estimates of K_p.

At 25 °C, where the 20 and 30% Chol were found to be in the two-phase L_o + gel region, we can consider how the location of the two phase boundaries is effected by a K_p in the range of $0.5 \le K_p \le 2$; ($K_p < 1$ favors the L_o phase over the gel phase in this case). This is illustrated in Figure 7, where *X* refers to the deviation of the gel boundary from 20% [Chol] and *Y* refers to that for the L_o boundary from 30% [Chol] as a function of the K_p in this range, using the results from our measurements at these two compositions. That is, we employed

$$\frac{[\text{mol \% of } L_o]}{[\text{mol \% of gel}]} = K_p \frac{P(L_o)}{P(\text{gel})} \qquad (1)$$

where $P(L_o)$ and $P(\text{gel})$ represent the measured relative populations of the two spectral components, as well as the lever rule for the ratio of [mol % of L_o]/[mol % of gel].[7,42] Figure 7 illustrates that there is only a modest variation in location of the phase boundaries predicted for this range of K_p values. For Figure 2, we used $X \cong Y \cong 1.63\%$, which corresponds to a $K_p \cong 0.8$ (i.e., slightly favoring the L_o phase), with some of the uncertainty in these boundaries shown in Figure 2, ascribable to the uncertainty in the precise value of K_p.

In the case of temperatures 48 and 57 °C, the phase boundaries were suggested to be close to the values of 10 and 30% [Chol], respectively, based on the similarity of the dynamic parameters found for their single-component spectra with those of the two components found for the 20% [Chol] spectrum. Once these phase boundaries were chosen, as shown in Figure 2, we estimated a K_p slightly greater than unity, indicating 16-PC favors the L_o phase slightly over the L_d phase.

Our study with 24 samples, while providing a useful overview of the phase diagram, would, in the future, require more experiments near the phase boundaries in order to refine their precise location. Then, for example, eq 1 and the lever rule could be used to accurately locate these boundaries as well as K_p,[7,42] and this determination could be supplemented by the use of the dynamic parameters, as has been illustrated in the above discussion.

Summary and Conclusions

An extensive 2D-ELDOR study of the model membrane system composed of binary mixtures of DPPC−cholesterol in excess water with 16-PC as the spin probe, over the temperature range of 25 to 57 °C and the composition range of pure DPPC and 0−50% [Chol], has enabled the characterization of the three phases present, gel, L_o, and L_d, in terms of their dynamical molecular properties, and it also enabled the construction of the phase diagram for this system.

The full Sc− method led to enhanced resolution, which enabled clear distinctions to be made between the spectra resulting from the three different phases present, despite the subtle differences in their properties. In general, the gel and L_o phases exhibited substantially greater ordering, S_0, than the L_d phase, and S_0 was modestly greater for the gel phase compared to that for the L_o phase. In the case of dynamics, $R_\perp$ exhibited the behavior $L_o > L_d >$ gel at the same temperature, and all increased with temperature. The 2D-ELDOR analysis allows the determination of other dynamic and ordering parameters ($R_\parallel$ and S_2), as well as other spin-relaxation parameters, such as T_2, T_1, and also the (Gaussian) inhomogeneous broadening. Both S_0 and T_{2edi}^{-1} (the extra line broadening not accounted for by rotational modulation of the hyperfine and g tensors) were found to be good indicators for distinguishing these phases. However, it is the normalized pure-absorption 2D-ELDOR contours in the SECSY mode (cf. Figure 5c) that most dramatically distinguished these phases.

The full Sc− method enabled the successful fitting of the 2D-ELDOR spectra in the two-phase regions and the unequivocal separation of the two spectral components. This could be used, in conjunction with the thermodynamic lever rule, to estimate the boundaries of the gel + L_o two-phase region at 25 °C, with just the minimum sufficient data points. Given more limited data at 48 and 57 °C, only rough estimates could be made of the boundaries of the $L_o + L_d$ two-phase region based on the similarity of the respective 2D-ELDOR spectral components with those from adjacent single-phase regions. In all of these cases, the ordering, dynamic, and spin-relaxation parameters could be used to confirm the assignments.

The DPPC−cholesterol phase diagram we determined, solely from the 2D-ELDOR results, is, in general, found to be in good agreement with those previously determined using several other methods, and we believe our results help to overcome the previous discrepancies obtained from the different methods.

This study, based on 24 samples of different composition and temperature, was sufficient to supply an overview of the phase diagram with somewhat rough estimates of the phase boundaries. Clearly, even more extensive studies focusing more on the phase boundary and two-phase regions would be needed to refine the phase diagram obtained in this study, and 2D-ELDOR is eminently suitable for such further studies.

A more thorough study by 2D-ELDOR of the two-phase regions, based on methods previously developed for cw-ESR,[7,42] can more accurately determine not only the phase boundaries but also the partition coefficient, K_p, in the respective phases. The present study benefited from the previous cw-ESR studies which showed a $K_p \sim 1$ in related lipid membrane systems. A complication in the study of coexisting phases in three-component model membranes, which are used to mimic biological membranes, is the need to experimentally determine the tie lines, which, however, are self-evident in two-component systems such as was studied in the present work. This task, which is a challenge for cw-ESR,[7,42] would also benefit from the greatly enhanced resolution of 2D-ELDOR using the full Sc− method.

Acknowledgment. This project was supported by Grant Number P41RR16292 from the National Center for Research Resources (NCRR) and Grant Number R01EB03150 from the National Institute of Biomedical Imaging and Bioengineering, components of the National Institute of Health (NIH), and its contents are solely the responsibility of the authors and do not necessarily represent the official views of NCRR or NIH. Computations were implemented at the Cornell Center for Materials Research for Computing Facility.

Supporting Information Available: Some of the spectral fits, obtained in the full Sc− fitting, are displayed as contours in the full Sc− domain. This material is available free of charge via the Internet at http://pubs.acs.org.

References and Notes

(1) Chiang, Y.-W.; Costa-Filho, A. J.; Freed, J. H. *J. Magn. Reson.* **2007**, *188*, 231.

(2) Chiang, Y.-W.; Costa-Filho, A. J.; Holowka, D.; Baird, B.; Freed, J. H. 2D-ELDOR for Biomembranes: Crosslinking IgE Receptors Causes Phase Structure Changes in Plasma Membrane Vesicles. **2007**, in preparation.

(3) Lagerholm, B. C.; Weinreb, G. E.; Jacobson, K.; Thompson, N. L. *Annu. Rev. Phys. Chem.* **2005**, *56*, 309.

(4) Kusumi, A.; Nakada, C.; Ritchie, K.; Murase, K.; Suzuki, K.; Murakoshi, H.; Kasai, R. S.; Kondo, J.; Fujiwara, T. *Annu. Rev. Biophys. Biomol. Struct.* **2005**, *34*, 351.

(5) Munro, S. *Cell* **2003**, *115*, 377.

(6) Ge, M.; Gidwani, A.; Brown, H. A.; Holowka, D.; Baird, B.; Freed, J. H. *Biophys. J.* **2003**, *85*, 1278.

(7) Swamy, M. J.; Ciani, L.; Ge, M.; Smith, A. K.; Holowka, D.; Baird, B.; Freed, J. H. *Biophys. J.* **2006**, *90*, 4452.

(8) Koynova, R.; Caffrey, M. *Chem. Phys. Lipids* **2002**, *115*, 107.

(9) Simon, S. A.; McIntosh, T. J. *Biochim. Biophys. Acta* **1991**, *1064*, 69.

(10) Karmakar, S.; Raghunathan, V. A. *Phys. Rev. E* **2005**, *71*.

(11) Sankaram, M. B.; Thompson, T. E. *Proc. Natl. Acad. Sci. U.S.A.* **1991**, *88*, 8686.

(12) Korlach, J.; Baumgart, T.; Webb, W. W.; Feigenson, G. W. *Biochim. Biophys. Acta* **2005**, *1668*, 158.

(13) Feigenson, G. W.; Buboltz, J. T. *Biophys. J.* **2001**, *80*, 2775.

(14) Huang, T. H.; Lee, C. W. B.; Dasgupta, S. K.; Blume, A.; Griffin, R. G. *Biochemistry* **1993**, *32*, 13277.

(15) Cao, H. H.; Zhang, J. B.; Jing, B. W.; Regen, S. L. *J. Am. Chem. Soc.* **2005**, *127*, 8813.

(16) Vist, M. R.; Davis, J. H. *Biochemistry* **1990**, *29*, 451.

(17) Ipsen, J. H.; Karlstrom, G.; Mouritsen, O. G.; Wennerstrom, H.; Zuckermann, M. J. *Biochim. Biophys. Acta* **1987**, *905*, 162.

(18) Xiang, T.-X.; Anderson, B. D. *Biochim. Biophys. Acta* **1998**, *1370*, 64.

(19) McMullen, T. P. W.; McElhaney, R. N. *Biochim. Biophys. Acta* **1995**, *1234*, 90.

(20) Chiang, Y.-W.; Shimoyama, Y.; Feigenson, G. W.; Freed, J. H. *Biophys. J.* **2004**, *87*, 2483.

(21) Borbat, P. P.; Crepeau, R. H.; Freed, J. H. *J. Magn. Reson.* **1997**, *127*, 155.

(22) Patyal, B. R.; Crepeau, R. H.; Freed, J. H. *Biophys. J.* **1997**, *73*, 2201.

(23) Costa-Filho, A. J.; Crepeau, R. H.; Borbat, P. P.; Ge, M.; Freed, J. H. *Biophys. J.* **2003**, *84*, 3364.

(24) Costa-Filho, A. J.; Shimoyama, Y.; Freed, J. H. *Biophys. J.* **2003**, *84*, 2619.

(25) Sastry, V. S. S.; Polimeno, A.; Crepeau, R. H.; Freed, J. H. *J. Chem. Phys.* **1996**, *105*, 5773.

(26) Gorcester, J.; Millhauser, G. L.; Freed, J. H. Two-Dimensional Electron Spin Resonance. In *Modern Pulsed and Continuous Wave Electron Spin Resonance*; Kevan, L., Bowman, M. K., Eds.; Wiley: New York, 1990; Chapter 3.

(27) Budil, D. E.; Lee, S.; Saxena, S.; Freed, J. H. *J. Magn. Reson., Ser. A* **1996**, *120*, 155.

(28) Schneider, D. J.; Freed, J. H. Calculating Slow Motional Magnetic Resonance Spectra. A User's Guide. In *Spin Labeling: Theory and Application*; Berliner, L. J., Reuben, J., Eds.; Plenum: New York, 1989; Vol. 8, p 1.

(29) Freed, J. H. Theory of Slow Tumbling ESR Spectra for Nitroxides. In *Spin Labeling: Theory and Applications*; Berliner, L. J., Ed.; Academic Press: New York, 1976; p 53.

(30) Lee, S. Y.; Budil, D. E.; Freed, J. H. *J. Chem. Phys.* **1994**, *101*, 5529.

(31) Buboltz, J. T.; Huang, J. Y.; Feigenson, G. W. *Langmuir* **1999**, *15*, 5444.

(32) Meirovitch, E.; Nayeem, A.; Freed, J. H. *J. Phys. Chem.* **1984**, *88*, 3454.

(33) Saxena, S.; Freed, J. H. *J. Magn. Reson.* **1997**, *124*, 439.

(34) Liang, Z.; Crepeau, R. H.; Freed, J. H. *J. Magn. Reson.* **2005**, *177*, 247.

(35) Gorcester, J.; Freed, J. H. *J. Chem. Phys.* **1988**, *88*, 4678.

(36) Freed, J. H.; Nayeem, A.; Rananavare, S. B. ESR and Slow Motions in Liquid Crystals. In *The Molecular Dynamics of Liquid Crystals*; Luckhurst, G., Veracini, C., Eds.; Kluwer: Dordrecht, The Netherlands, 1994; p 365.

(37) Schwartz, L. J.; Stillman, A. E.; Freed, J. H. *J. Chem. Phys.* **1982**, *77*, 5410.

(38) Gorcester, J.; Millhauser, G. L.; Freed, J. H. Two-Dimentional Electron Spin Resonance. In *Modern Pulsed and Continuous Wave Electron Spin Resonance*; Kevan, L., Bowman, M. K., Eds.; Wiley: New York, 1990.

(39) Crepeau, R. H.; Saxena, S.; Lee, S.; Patyal, B.; Freed, J. H. *Biophys. J.* **1994**, *66*, 1489.

(40) Saxena, S.; Freed, J. H. *J. Phys. Chem. A* **1997**, *101*, 7998.

(41) Fresch, B.; Frezzato, D.; Moro, G. J.; Kothe, G.; Freed, J. H. *J. Phys. Chem. B* **2006**, *110*, 24238.

(42) Chiang, Y.-W.; Zhao, J.; Wu, J.; Shimoyama, Y.; Freed, J. H.; Feigenson, G. W. *Biochim. Biophys. Acta* **2005**, *1668*, 99.